History of Medicine Studies
ISSN:1300-669
Volume 20 Issue 1 June 2024

An analysis of the cynomolgus monkey pharmacokinetic-pharmacodynamic model of the monoclonal anti-macaque-IL-15 antibody Hu714MuXHu

[1] DR M GOVARDHAN,[2]Dr. B. ARUNA,[3] R. JONA METHUSULA,
[4]S SHAHEENA BEGUM,[5]K. ANJANEYULU,[6]DR SATRASALA NEELIMA
Department of Pharmacology, Dr K.V Subba Reddy Institute of Pharmacy

Abstract
IL-15 is a proinflammatory cytokine that has been linked to the development of inflammatory illnesses and is involved in the activation of memory CD8+ and natural killer (NK) T-cells; the recombinant chimeric murine-human monoclonal antibody Hu714MuXHu targets this cytokine. To explain the decrease in NK cell count in cynomolgus monkeys treated with Hu714MuXHu, a pharmacokinetic-pharmacodynamic (PK/PD) model was created. In three separate investigations, cynomolgus monkeys were given Hu714MuXHu doses: with a single intravenous dosage of 0.1 or 1 mg kg—1; once weekly for five weeks at 0, 30, 60, or 150 mg kg—1 i.v.; or 150 mg kg—1 subcutaneously; once weekly for thirteen weeks at 0, 5, 30, or 150 mg kg—1 subcutaneously. Medicated serum

We used noncompartmental analysis to examine the concentration-time data of Hu714MuXHu, and simultaneous PK/PD modeling to evaluate the link between NK cell count and PK. PK of Hu714MuXHu was dose-proportional when administered intravenously (0.1-150 mg·kg—1) and systemically (5-150 mg·kg—1), with an elimination half-life ranging from 12.7 to 18 days. After the first treatment, the serum Hu714MuXHu concentrations reached 0.1 lg·mL—1, the limit of quantification for the experiment, and the NK cell numbers returned completely. An EC50 of 0.09 lg·mL—1 was observed in the PK/PD model of Hu714MuXHu's effects on NK cells. In conclusion, cynomolgus monkeys were shown to exhibit linear PK and a substantial decrease in NK cell count after receiving weekly intravenous or subcutaneous doses of Hu714MuXHu for a maximum of three months, as indicated by PK/PD models. In cases of inflammatory disorders where changes in NK cell count are measurable, this method could help direct the selection of doses for investigational products.
Short Forms
Laboratory Animal Care International's Assessment and Accreditation Commission (AAALAC); C0 is the serum concentration extended to time zero; CD is the cluster of differentiation; CL is the clearance in serum; BSV is the between-subject variability; Ab is the antibody; AUMC is the area under the serum concentration-time curve; and CL is the acronym for "clearance in serum." Serum concentration at its greatest observed value (Cmax); maximal electrolyte concentration (Emax)

History of Medicine Studies
ISSN:1300-669
Volume 20 Issue 1 June 2024

Introduction

In response to innate immune stimuli and type 1 interferons (IFN), dendritic cells, monocytes, macrophages, epithelial cells, fibroblastic cells, and bone marrow stromal cells primarily produce interleukin-15 (IL-15), a powerful proinflammatory cytokine structurally similar to IL-2 (Fehniger and Caligiuri 2001). A heteromeric receptor complex including the IL-15R a chain, the common c chain, and the IL-2/15R b chain binds to the IL-15 signal. Memory CD8+ T cells, natural killer (NK) cells, and NK T cell development, differentiation, and proliferation are all facilitated by interleukin (IL)-15, which operates on many immune cells (Grab-stein et al. 1994; Waldmann and Tagaya 1999). Additionally, dendritic cells are better able to survive and activate when exposed to IL-15 (Mattei et al., 2001; Gil et al., 2010). Early in inflammatory diseases, IL-15 recruits and activates inflammatory cells, which in turn increases the production of proinflammatory cytokines such IFNc and tumor necrosis factor a (TNFa) (McInnes et al. 1997; Musso et al. 1998).

Increased levels of IL-15 in peripheral blood and tissue have been demonstrated in a variety of autoimmune inflammatory disease including rheumatoid arthritis (McInnes et al. 1997; Gonzalez-Alvaro et al. 2003, 2011), systemic lupus erythematosus (Baranda et al. 2005), psori- asis (D'Auria et al. 1999; Ong et al. 2002), and celiac dis- ease (Maiuri et al. 2000; De Nitto et al. 2009; Meresse et al. 2012; Abadie and Jabri 2014), as well as graft-versus- host disease, and solid organ transplant rejection (Smith et al. 2002), suggesting that IL-15 plays a critical role in the pathogenesis of these diseases or conditions. Some inflammatory diseases and autoimmune disorders may be treatable with the suppression of IL-15, which is thought to decrease the inflammatory response. Inhibitors of IL-15 activity have been reported in several publications. Antibodies targeting IL-15 have shown efficacy in a mouse model containing human psoriasis xenografts, and neutralization of IL-15 via the soluble IL-15 receptor or blocking of the IL-15 receptor improved collagen-induced arthritis in mice (Ruchatz et al. 1998; Villadsen

from 2003 by et al. and 2004 by Ferrari-Lacraz et al. Moreover, blockage of IL-15 in a celiac disease model in mice resulted in intraepithelial lymphocyte apoptosis, decreased accumulation in the gut epithelium, and prevented proinflammatory signaling in human celiac disease biopsies (Benahmed et al. 2007; Malamut et al. 2010).

The crucial function of IL-15 in NK cell growth and maintenance has been shown by data obtained from preclinical animals. NK cell counts are decreased in IL-15 and IL-15Ra knockout mice (Lodolce et al. 1998; Kennedy et al. 2000), but NK cell numbers may be restored in IL-15 knockout mice by exogenous IL-15 treatment (Kennedy et al. 2000). A decrease in the number of NK cells in the peripheral blood was seen in cynomolgus monkeys when the IL-15 receptor was blocked (Haustein et al. 2010). In a similar vein, cynomolgus monkeys had their NK cell numbers decreased when given tofacitinib (CP-690,550), an inhibitor of Janus kinase 3 (JAK3) that prevents signals from reaching certain cytokine receptors, such as IL-15 (Conklyn et al. 2004). Nevertheless, it does not seem that IL-15 is necessary for the maintenance of human NK cells, even if it may play a significant role in their development (Grabstein et al. 1994; Waldmann and Tagaya 1999). (Lebrec et al. 2013).

Our team has created a monoclonal antibody called AMG 714 that targets human immunoglobulin G1 (IgG1j) and blocks its activities. While AMG 714 bound human IL-15 strongly, it bound macaque IL-15 less strongly, according to in vitro research. Furthermore, AMG 714 effectively blocked human IL-15 but had no such effect on macaque IL-15. Through the fusion of the antibody-binding part [F(ab)] of a mouse anti-human IL-15 monoclonal antibody (M111), which is known to

neutralize macaque IL-15, with a human IgG1 constant region (Fc), a surrogate antibody, Hu714MuXHu, was produced to allow for preclinical research in macaques. The neutralizing efficacy of Hu714MuXHu against macaque IL-15 was found to be comparable to that of AMG 714 against human IL-15 in vitro.
Our research aimed to predict the PK and its effects on NK cell count, as well as to learn about the pharmacodynamics and pharmacokinetics.

after single or multiple Hu714MuXHu intravenous (i.v.) or subcutaneous (s.c.) administration in male and female cynomolgus monkeys. To our knowledge, this is the first report on the PK/PD modeling of an anti-IL-15 antibody. However, because the reduction in NK cell counts in cynomolgus monkeys was not observed in healthy humans after administration of AMG 714, the utility of our PK/PD model might be restricted to certain clinical disease conditions. For example, although survival of human NK cells is IL-15 independent (Lebrec et al. 2013), a recent study in cancer patients demonstrated influx and hyperproliferation of NK cells in the peripheral blood after IL-15 administration (Conlon et al. 2015). These data suggest that IL-15 blockade might only affect NK cell counts under conditions where IL-15 levels are elevated (e.g., in patients with inflammatory diseases). In addition, the presented PK/PD modeling approach may be useful for guiding therapeutic dose selection of investi- gational agents that target the IL-15 pathway such as JAK3 inhibitors (Conklyn et al. 2004; Borie et al. 2005).

Materials and Methods

Test material

Hu714MuXHu (molecular weight: 144 kDa) is a chimeric monoclonal antibody with a murine variable region grafted on a human IgG_1 constant region. It is a surrogate for the fully human monoclonal antibody AMG 714, which is directed against human IL-15. Hu714MuXHu binds to cynomolgus monkey and human IL-15 with comparable affinity, with K_D values of 120 60 pmol*L^{-1} and 240 40 pmol*L^{-1}, respectively. Hu714MuXHu and AMG 714 bind to overlapping epitopes on human IL-15 and do not interfere with IL-15 binding to IL-15 receptor
a. Instead, they prevent IL-15 signaling by blocking assembly of the complete receptor complex. However, whereas AMG 714 does not efficiently neutralize cynomolgus monkey IL-15, Hu714MuXHu does, and has thus been used for preclinical testing in cynomolgus mon- keys.

The investigational product was formulated with phar- maceutically accepted excipients at a nominal concentra- tion of 30 mg·$mL^{—1}$ and stored at —60 to —80°C until use. At least 24 h prior to dose preparation, the test arti- cle was transferred to a refrigerator at 2–8°C. The control article was formulated with the same excipients and stored at 2–8°C.

Animal husbandry

Na€ıve male (N = 55) and female (N = 49) cynomolgus monkeys (*Macaca fascicularis*) of Chinese origin (N = 104 total, age: 3–6 years, weight: 2.0–4.6 kg) were obtained for the conduct of the studies. Experiments were performed in facilities accredited by the Associa- tion for Assessment and Accreditation of Laboratory Animal Care International (AAALAC; Frederick, MD). The experiments were conducted in compliance with the most recent version of the United States Food and Drug Administration (US FDA) Good Laboratory Practice Regulations, 21 CFR part 58; the Japanese Ministry of Health, Labor, and Welfare (MHLW), Good Laboratory Practice (GLP) Standards, Ordinance 21; the Organiza- tion for Economic Cooperation and Development (OECD) Principles of GLP, C(97) 186/Final; and with any applicable amendments. This research also adhered to the “Principles of Laboratory Animal Care” (US National Institute of Health Publication #85-23, revised in 1985). Results obtained from animal studies have been reported in accordance with the ARRIVE guidance (Kilkenny et al. 2010).

The monkeys were acclimated to laboratory conditions for at least 4 weeks and housed individually in stainless- steel cages, except when comingled for environmental enrichment unless precluded for behavior or health rea- sons. The environment was maintained within a tempera- ture range 18–29°C, relative humidity range 30–70%, 10 or greater air changes/hour and a 12-h light/dark cycle. Unless fasted, certified primate diet was available ad libi- tum two times daily; purified tap water was available ad li- bitum. Fruits, vegetables, and toys were given as a form of environmental enrichment.

Dose administration

History of Medicine Studies
ISSN:1300-669
Volume 20 Issue 1 June 2024

Serum Hu714MuXHu concentration-time and pharmaco- dynamic data for the current manuscript were obtained from three studies in cynomolgus monkeys: a single-dose PK and PD study and 1-month (5 weekly doses) and 3- month (13 weekly doses) GLP toxicology studies. The test article was administered to cynomolgus monkeys based on body weight as a single-dose i.v. administration into the saphenous vein, or once-weekly for 1 or 3 months via i.v. or s.c. in a saphenous vein or the dorsal thoracic region, respectively.

PK, PD, and immunogenicity assessments

Pre- and postdose blood samples for PK and PD measure- ments were collected as summarized in Table 1. Animals were not fasted for sample collections (unless the collec- tion was concurrent with clinical pathology sampling).

For the determination of serum Hu714MuXHu con- centrations, blood samples were collected via the femoral vein into plain tubes with no anticoagulant. Blood sam-

Table 1. Hu714MuXHu treatments and procedures for studies in cynomolgus monkeys.

Study	*N*	Groups	Treatment	Blood sample collection for PK	Blood sample collection for PD[1]
Single dose	6 males	2 groups; 3 per group	0.1 mg·kg^{-1} i.v. 1 mg·kg^{-1} i.v. Single dose	Predose, and on Days 3, 5, 8, 14, 21, 28, 35, and 42	2 times at baseline; predose, and on Days 3, 5, 8, 14, 21, 28, 35, and 42
1-month GLP	25 males 25 females	5 groups; 5 per sex per group	Vehicle control i.v. 30 mg·kg^{-1} i.v. 60 mg·kg^{-1} i.v. 150 mg·kg^{-1} i.v. 150 mg·kg^{-1} s.c. QW for 4 weeks	Predose, and 0.5, 2, 8, 24, 96, and 168 h postdose on Days 1 and 22, and predose on Day 15. In recovery monkeys (2/sex per group), on Days 43, 57, 71, 85, 113, 141, 169, 197, 225, 253, 281, 309, and 337	2 times at baseline, predose on Day 15, and on Day 30. In recovery monkeys, on Days 57, 85, 113, 141, 169, 197, 225, 253, 281, 309, and 337
3-month GLP	24 males 24 females	4 groups; 6 per sex per group	Vehicle control s.c. 5 mg·kg^{-1} s.c. 30 mg·kg^{-1} s.c. 150 mg·kg^{-1} s.c. QW for 13 weeks	Predose, and 0.5, 2, 8, 24, 48, and 168 h postdose on Day 1. Predose, and 0.5, 2, 8, 24, 96, and 168 h postdose on Day 85. Predose on Days 29 and 57 and 1 day after day 92 dose. In recovery monkeys (2/sex/group), on Days 106, 120, 134, 148, 176, and 205	3 times at baseline; predose 1 and on Day 3; predose on Days 8, 15, 29, and 57 and on Day 93. In recovery monkeys, on Days 120, 148, 176, and 205

i.v., intravenously; s.c., subcutaneously; PD, pharmacodynamics; PK, pharmacokinetics; QW, once-weekly.
[1]PD assessment via immunophenotyping.

ples were allowed to clot for at least 1 h (but not longer than 4 h); after centrifugation at 2000*g* for 10 min, serum was aliquoted, stored at —60 to —80°C and subsequently shipped to Amgen Inc. for analysis. Serum samples from the three studies were analyzed for Hu714MuXHu using a validated quantitative enzyme-linked immunosorbent assay (ELISA) with a lower limit of quantification (LLOQ) of 0.1 *l*g·mL^{-1}. Briefly, microplate wells were coated with monoclonal anti-Hu714MuXHu antibody to capture Hu714MuXHu. Standard and quality control samples, made by spiking Hu714MuXHu into 100% cynomolgus monkey serum, as well as blanks and study samples were loaded into the microplate wells after a dilution of 1:100 with buffer. Following incubation, unbound material was removed by washing. The detec- tion reagent, biotinylated polyclonal anti-Hu714MuXHu, was then added to the wells. After removal of the unbound biotinylated antibody by washing, streptavidin conjugated poly-horseradish peroxidase (HRP; Thermo, IL) was added to each well. After another washing step, a tetramethylbenzidine solution (Bio FX Laboratories, MD) was added to the wells. After stopping the color develop- ment, the optical density was measured at 450–650 nm. Data were reduced using the Watson version 7.0.0.01 data reduction package using a 5-parameter (auto estimate) regression model.

History of Medicine Studies
ISSN:1300-669
Volume 20 Issue 1 June 2024

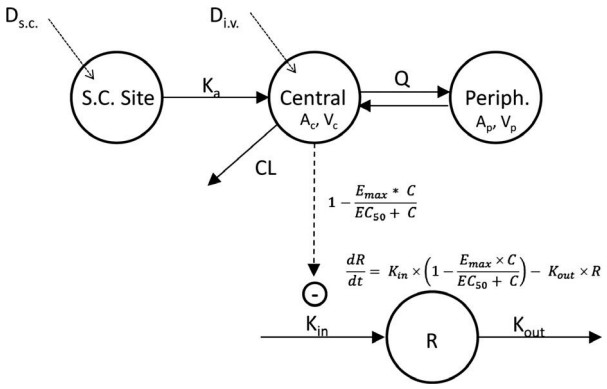

Figure 1. Simultaneous PK/PD modeling of Hu714MuXHu in cynomolgus monkeys: $D_{s.c.}$ and $D_{i.v.}$ are subcutaneous and intravenous doses, respectively; K_a is the absorption rate constant after s.c. administration; CL is the linear elimination clearance from the central compartment; Q is the inter-compartmental clearance between the central and peripheral compartments; A_c, V_c and A_p, V_p are central and peripheral amount and volume of distribution for Hu714MuXHu. Hu714MuXHu concentration in the central compartment $C = A_c/V_c$. R is the number of NK cells 9 $10^3 \cdot l L^{-1}$ of blood with a baseline value of R_0. NK cell turnover rate dR/dt is described by production (K_{in}) and loss (K_{out}) rate constants with Hu714MuXHu concentration in the central compartment inhibiting NK cell production. E_{max} is the maximal effect, EC_{50} is the concentration producing 50% of the maximal effect. Pheriph, peripheral compartment.

well just prior to the addition of the acid-treated serum samples. The serum samples, at neutral pH, were mixed and left at room temperatures to allow anti- Hu714MuXHu antibodies to bind to the covalently attached Hu714MuXHu. The plate was washed with wash buffer and peroxidase-conjugated streptavidin was added to each well. The plate was washed again and a tetram- ethylbenzidine substrate solution was added for color development. The enzymatic reaction was stopped with phosphoric acid and the plate was read on a calibrated spectrophotometer to determine the optical density of each well. The LLOQ was 0.25 $l g \cdot mL^{-1}$ in the presence of 10 $l g \cdot mL^{-1}$ of Hu714MuXHu in cynomolgus serum.

PK analysis and PK/PD modeling

Noncompartmental analyses were performed using WinNonlin® Version 4.1e (Pharsight®, a Certara® Com- pany, Sunnyvale, CA) to determine the following PK parameters after single or multiple i.v. or s.c. administra- tions: observed maximum concentration in serum after

(AUC_∞, for single dosing), and total body clearance (CL for single i.v. dosing). The rate constant for the terminal log-linear phase of the concentration-time curve (k_z) was estimated using linear regression. The terminal phase elimination half-life ($t_{1/2}$) was calculated as $\ln 2/k_z$. For the single dose study, volume of distribution at steady state (V_{ss}) was calculated as V_{ss} = CL 9 MRT with MRT being the mean residence time calculated as MRT = $AUMC_\infty$/ AUC_∞, where $AUMC_\infty$ is the area under the first- moment-time curve extrapolated to infinity.

Simultaneous PK/PD modeling was performed using NONMEM® software version VII (ICON Development Solutions, Ellicott City, MD) with the gfortran FORTRAN compiler. The PK/PD model was used to fit the data to characterize the PK properties and the PK-PD relation- ship of Hu714MuXHu in cynomolgus monkeys. The structure of the final PK/PD model is shown in Figure 1. The PK was characterized by a two-compartment model with linear elimination from the central compartment. The PD effect of Hu714MuXHu on NK cells was described by an indirect response model:

s.c. (C_{max}) and extrapolated to time zero after i.v. (C_0)

$$\frac{dR}{dt} = K_{in} \times \left(1 - \frac{E_{max} \times C}{EC + C}\right) - K_{out} \times R$$

administration, time to C_{max} (t_{max}), area under the serum Hu714MuXHu concentration-time curve calculated using the linear/log trapezoidal rule within the dosing interval (AUC_s, for multiple dosing) or extrapolated to infinitywhere R is the number of NK cells 9 $10^3 \cdot l L^{-1}$ in blood with a baseline value of R_0, C is the Hu714MuXHu con-

50

History of Medicine Studies
ISSN:1300-669
Volume 20 Issue 1 June 2024

Table 2. Mean (SD) Hu714MuXHu noncompartmental pharmacokinetic parameters.

Single dose	N = 4/Group	0.1 mg·kg^{-1} i.v.	1 mg·kg^{-1} i.v.
	C_0 (μg·mL^{-1})	1.65 (0.16)	17.9 (7.76)
	AUC$_\infty$ (μg·day·mL^{-1})	27.2 (4.20)	293 (76.1)
	CL (mL·day^{-1}·kg^{-1})	3.73 (0.56)	3.54 (0.80)
	V_{ss} (mL·kg^{-1})	67.9 (9.6)	77.2 (22.8)
	$t_{1/2}$ (day)	12.7 (0.57)	15.3 (1.3)

1-month GLP	N = 10/Group	30 mg·kg^{-1} QW i.v.	60 mg·kg^{-1} QW i.v.	150 mg·kg^{-1} QW i.v.	150 mg·kg^{-1} QW s.c.
Day 1	C_0 or C_{max} (μg·mL^{-1})	878 (103)	1700 (94.6)	3350 (346)	1560 (203)
	AUC$_s$ (μg·day·mL^{-1})	3130	(368) (344) 585 (1070)	12200	9100 (1280)
	C_0 or C_{max} (μg·mL^{-1})	1490	(172) (380) 276	5740 (468)	3640 (489)
Day 22	AUC$_s$ (μg·day·mL^{-1})	7210	(1080) (1280) 12,90	25,300 (2780)	23,900 (3300)
	$t_{1/2}$ (day)	15 (4)	16 (1)	17 (1)	16 (4)

3-month GLP	N = 12/group	5 mg·kg^{-1} QW s.c.	30 mg·kg^{-1} QW s.c.	150 mg·kg^{-1} QW s.c.
Day 1	C_{max} (μg·mL^{-1})	53.5 (4.8)	355 (60)	1400 (212)
	AUC$_s$ (μg·day·mL^{-1})	310 (36)	2050 (343)	8450 (1260)
	C_{max} (μg·mL^{-1})	176 (25)	1090 (172)	4370 (545)
Day 85	AUC$_s$ (μg·day·mL^{-1})	1180 (169)	7130 (1170)	28,500 (3880)
	$t_{1/2}$ (day)	18 (2)	16 (2)	16 (4)

i.v., intravenously; s.c., subcutaneously; QW, once-weekly; C_{max}: maximum observed concentration for s.c.; C_0, extrapolated concentration at time zero for i.v.; AUC$_s$, area under the concentration-time curve within the 7-day dosing interval on Days 1, 22, or 85; AUC$_\infty$, area under the concen- tration-time curve from time zero extrapolated to infinity; CL, clearance in serum after i.v. administration; $t_{1/2}$, elimination half-life; V_{ss}, volume of distribution at steady state after i.v. administration.

centration in the central compartment, E_{max} is the maximal effect, EC_{50} is the concentration producing 50% of the maximal effect, and K_{in} and K_{out} are the forma- tion and elimination rate constants of NK cells, respec- tively. Based on the biology, the effect of Hu714MuXHu concentration on the NK cell population was assumed to be the inhibition of the formation (K_{in}) of the NK cells.

Data from all three studies were fitted simultaneously with the NONMEM® ADVAN13 subroutine using the first-order conditional estimation method with INTER- ACTION (FOCEI) followed by Monte Carlo Importance Sampling (IMP) method and covariance step with MATRIX = S to estimate population PK and PD parame- ters and to obtain standard error estimates for each parameter. Because log-normal distribution was assumed for between-subject variability (BSV), exponential models were used to describe the BSV in the model parameter estimates: P_i = TVP·exp(g), where P_i is the individual

History of Medicine Studies
ISSN:1300-669
Volume 20 Issue 1 June 2024

model parameter for the *i*th subject, TVP is the typical value of the parameter value P, and *g* is a normally dis- tributed random variable with mean of zero and an unknown variance x^2 to be estimated. Correlation between BSV of CL and *V* was also considered in the model. The residual variability was first modeled assum- ing an additive and proportional error model,
$Y = F\ 9\ (1 + e_1) + e_2$, where *Y* is the PK or PD observa- tion, *F* represents the model prediction values and e_1 and e_2 are normally distributed random variables with mean of zero and unknown variance. The additive error e_2 was fixed to zero in the final model due to its value being consistently estimated to be near zero during model development.

Graphical analyses were performed using R version 3.0.0 for Windows (R project, http://www.r-project.org/) or SigmaPlot version 12.5 (Systat Software, San Jose, CA). Model selection was guided by visual inspection of standard goodness-of-fit plots, parameter estimate

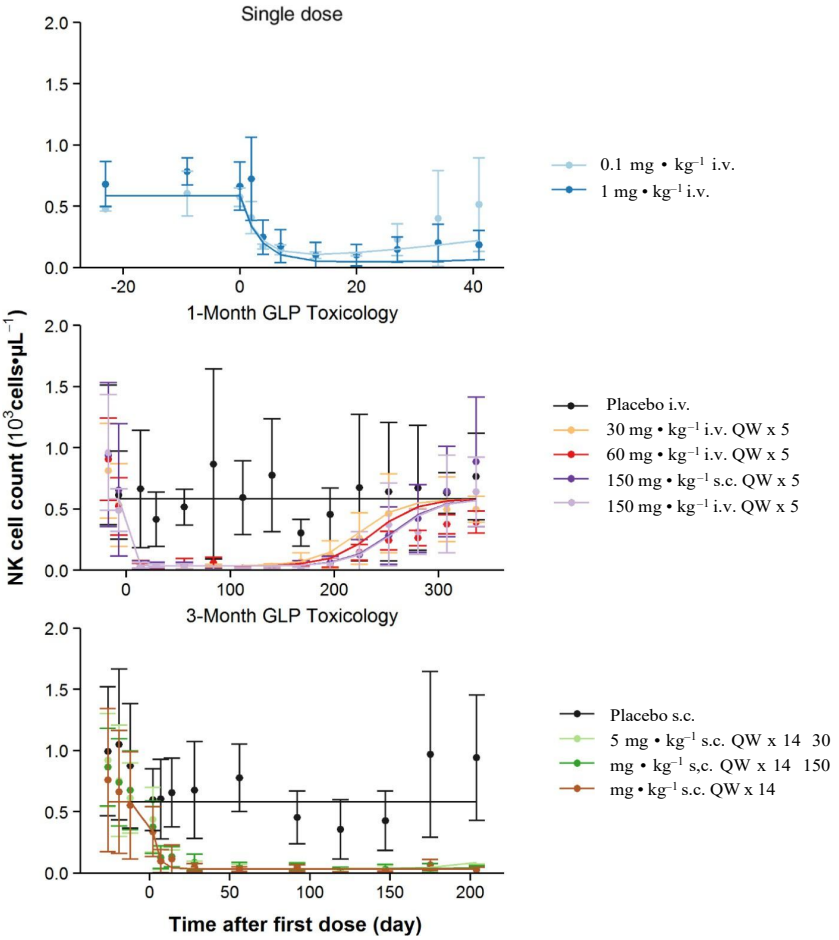

Figure 3. Observed (symbols; mean SD) and population predicted (lines) NK cell count-time profiles after single and multiple i.v. or s.c. administration of Hu714MuXHu in cynomolgus monkeys.

precision/plausibility, visual predictive check (VPC), and shrinkage of empirical Bayes estimates (Brendel et al. 2007).

Results

Pharmacokinetics and immunogenicity response

Weekly i.v. or s.c. dosing with Hu714MuXHu for up to 3 months in cynomolgus monkeys was well tolerated (data on file at Amgen Inc.). Figure 2 shows the by-study and by-cohort observed mean (SD) and population predicted serum Hu714MuXHu concentration versus time profiles after single or multiple i.v. or s.c. dosing. The curvature for the

History of Medicine Studies
ISSN:1300-669
Volume 20 Issue 1 June 2024

observed data (symbols) around Day 300 was due to data from less animals (N = 2/co- hort), which did not follow the preceding general data trend of a typical linear two-compartment model. Note that, on an individual basis, those animals had PK profiles that did not display curvature around Day
300 (data on file at Amgen Inc.). Table 2 summarizes the estimated noncompartmental Hu714MuXHu PK parameters. Across the studied dose range (0.1– 150 mg·kg^{-1}), Hu714MuXHu exhibited linear kinetics; the exposure parameters C_{max} and AUC$_s$ of Hu714MuXHu increased approximately dose-proportion- ally both when administered as i.v. and as s.c. injections. Based on Day 1 AUC$_s$ values, a relative bioavailability of 65% and 75% was calculated for the 30 and 150 mg·kg^{-1}
s.c. dose cohorts, respectively, compared to those of the corresponding i.v. dose cohorts. In all three studies, no

K_a (day^{-1})	0.522 (7.11)	23.7 (38.6)
CL (mL·day^{-1}·kg^{-1})	3.66 (3.22)	17.1 (19.8)
V_c (mL·kg^{-1})	44.8 (4.51)	15.2 (35.7)
Q (mL·day^{-1}·kg^{-1})	5.07 (17.9)	72.1 (52.9)
V_p (mL·kg^{-1})	24.3 (8.25)	12.6 (126)

and survival of NK cells. The effect of Hu714MuXHu on NK cell counts are presented as mean (SD) profiles in Figure 3. Administration of Hu714MuXHu to cynomol- gus monkeys resulted in a rapid decline in NK cell counts. NK cell counts returned to predose baseline at 41 days after single 0.1 mg·kg^{-1} i.v. dosing; only partial return to baseline at 336 days after the first dose for all 1-month study active dose cohorts was observed. Due to the limited durations of the follow-up period, the NK cell count reduction did not reach predose baseline 41 days after single 1 mg·kg^{-1} i.v. dose or 204 days after the first dose for any of the 3-month study active dose cohorts.

Population PK/PD modeling

A total of 1408 Hu714MuXHu concentration versus time data points and 982 PD (NK cell count) versus time data points from 104 monkeys were included in the simultane- ous PK/PD modeling analyses. The final population parameter estimates and between-subject variability (BSV) of the PK/PD model are presented in Table 3. The popu- lation typical values for clearance (CL) and central vol- ume of distribution (V_c) were 3.66 mL·day^{-1}·kg^{-1} and
44.8 mL·kg^{-1}, respectively, consistent with what was
expected due to the high-molecular weight of Hu714MuXHu.

Table 3. Population PK/PD model parameter estimates for Hu714MuXHu.

Parameter

History of Medicine Studies
ISSN:1300-669
Volume 20 Issue 1 June 2024

anti-Hu714MuXHu antibodies were detected in any of the serum samples.

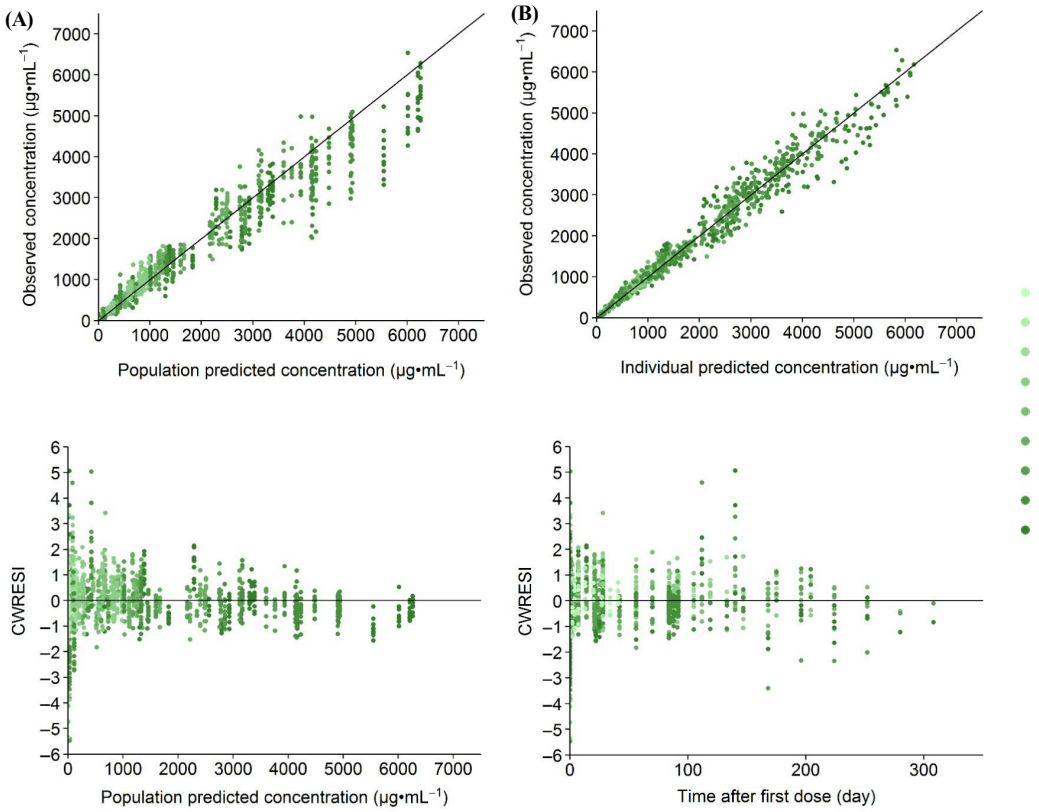

History of Medicine Studies
ISSN:1300-669
Volume 20 Issue 1 June 2024

(C) (D)

0.1 mg • kg^{-1}i.v. 1 mg • kg^{-1}i.v.
5 mg • kg^{-1}s.c. QW x 14 30 mg • kg^{-1}s,c. QW x 14 30 mg • kg^{-1}i.v. QW x 5 60 mg • kg^{-1}i.v. QW x 5
150 mg • kg^{-1}s.c. QW x 14 150 mg • kg^{-1}s.c. QW x 5 150 mg • kg^{-1}i.v. QW x 5

Figure 4. Goodness-of-fit plots for Hu714MuXHu concentrations: the observed Hu714MuXHu concentrations were plotted against the population predicted concentrations (A) and the individual predicted concentrations (B). The calculated conditional weighted residuals with interaction (CWRESI) were plotted against the population predicted concentrations (C) and time after first dose (D).

The first-order loss of response (K_{out}) was estimated to be 0.305 day^{-1} translating into a half-life of 2.27 days. The estimated values for E_{max}, EC_{50}, and the baseline R_0 were 0.941 9 10^3 cells·*l*L^{-1}, 0.0978 *l*g·mL^{-1}, and 0.584 9 10^3 cells·*l*L^{-1}, respectively. For all model-estimated PK and PD parameters, the relative standard errors (%RSE) were below 30% suggesting that these parameters were estimated with good precision. As Figures 2 and 3 demonstrate, the structural two-compartment PK/PD model with linear elimination from the central compart- ment and the E_{max} indirect response model adequately describe the serum concentration-time profiles of Hu714MuXHu and its effects on NK cell counts for all tested dose levels. Based on the goodness-of-fit plots, there was a good agreement between the predicted and observed individual data, and no systematic bias was identified in the diagnostic plots of the final model (Figs. 4, 5). Results of the VPC with 500 datasets simu- lated based on the final PK/PD model parameter esti- mates are shown in Figures 6 and 7. These plots again demonstrated that the estimated medians and the two- sided 90% confidence intervals (5th, 50th, and 95th percentiles) of the simulated Hu714MuXHu concentra- tion versus time and NK cell count versus time profiles contain the majority of the individual PK and PD observations.

Discussion and Conclusions

Interleukin-15 is an important proinflammatory cytokine that is implicated in the pathogenesis of autoimmune dis- eases including rheumatoid arthritis (McInnes et al. 1997; Gonzalez-Alvaro et al. 2003, 2011), systemic lupus erythe- matosus (Baranda et al. 2005), psoriasis (D'Auria et al. 1999; Ong et al. 2002), and celiac disease (Maiuri et al. 2000; De Nitto et al. 2009). Because multiple immune cells such as CD8+ T cells and NK cells depend on IL-15 for development, differentiation, and proliferation, blockade of IL-15 activity has been suggested as a possible treatment strategy for several of the aforementioned autoimmune dis- eases. We have evaluated the PK and PD of Hu714MuXHu, a recombinant chimeric murine-human antibody that specifically binds to macaque IL-15, and developed a PK/ PD model to describe the relationship between serum

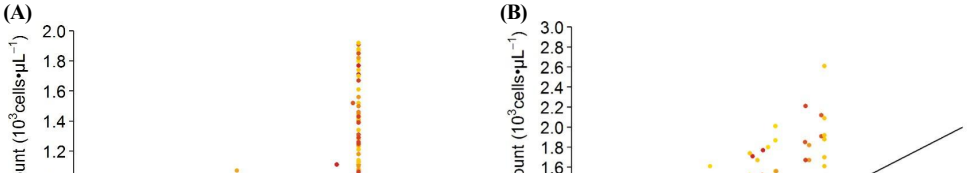

History of Medicine Studies
ISSN:1300-669
Volume 20 Issue 1 June 2024

(C) **(D)**

Placebo i.v. Placebo s.c.
0.1 mg • kg^{-1}i.v. 1 mg • kg^{-1}i.v.
5 mg • kg^{-1}s.c. QW x 14
30 mg • kg^{-1}s,c. QW x 14 30 mg • kg^{-1}i.v. QW x 5 60 mg • kg^{-1}i.v. QW x 5
150 mg • kg^{-1}s.c. QW x 14 150 mg • kg^{-1}s.c. QW x 5 150 mg • kg^{-1}i.v. QW x 5

Figure 5. Goodness-of-fit plots for NK cell counts after administration of Hu714MuXHu: the observed NK cell counts were plotted against the population predicted NK cell counts (A) and the individual predicted NK cell counts (B). The calculated conditional weighted residuals with interaction (CWRESI) were plotted against the population predicted NK cell counts (C) and time after first dose (D).

History of Medicine Studies
ISSN:1300-669
Volume 19 Issue 1 June 2023

Hu714MuXHu concentrations and reduction in NK cell counts after single i.v. or multiple i.v. or s.c. administra- tions to cynomolgus monkeys.

Hu714MuXHu PK in cynomolgus monkeys after a sin- gle dose i.v. or after weekly i.v. or s.c. doses for up to 3 months was linear within the investigated dose range of 0.1 to 150 mg·kg^{-1}. The similar mean terminal elimination half-life ($t_{1/2}$) of 12.7–18 days across the inves- tigated doses and duration, as well as two different routes of administration, suggest that the elimination characteris- tics of Hu714MuXHu were dose-, time-, and administra- tion route-independent. The observed accumulation of Hu714MuXHu in the 1- and 3-month studies is consistent with the long half-life of this monoclonal antibody. No immunogenicity response (anti-Hu714MuXHu antibodies) or sex differences were observed.

Consistent with results from previously published stud- ies using tofacitinib (CP-690550), a JAK3 inhibitor that inhibits signal transduction of the common *c* chain of cytokine receptors, including IL-15 (Conklyn et al. 2004; Borie et al. 2005), administration of Hu714MuXHu reduced NK cell numbers in cynomolgus monkeys.

Simultaneous PK/PD modeling using all individual animal data of three studies and all dosing regimens was adequate, with predicted PK parameters matching well with those obtained using noncompartmental analysis. The model-estimated population values for clearance (CL) and central volume of distribution (V_c) were 3.66 mL·day^{-1}·kg^{-1} and 44.8 mL·kg^{-1}, respectively, indi- cating slow elimination and limited tissue penetration and predominant distribution in serum (central compartment) as expected for this high-molecular weight protein (Ng et al. 2006; Dirks and Meibohm 2010; Royer et al. 2010).

The PD activity of Hu714MuXHu measured as NK cell count reduction following single or multiple doses was adequately described by the PK/PD model. The rapid decrease in NK cell numbers after Hu714MuXHu admin- istration is consistent with reports in mice, where NK cells transferred into mice with IL-15 deficiency were lost rapidly. This suggests that macaque NK cell survival is also dependent on IL-15 signaling (Koka et al. 2003; Prlic et al. 2003; Jamieson et al. 2004). In mice, the half-life of NK cells after transfer into wild-type mice was 7 days compared to only approximately 10 h in IL-15R$a^{-/-}$mice

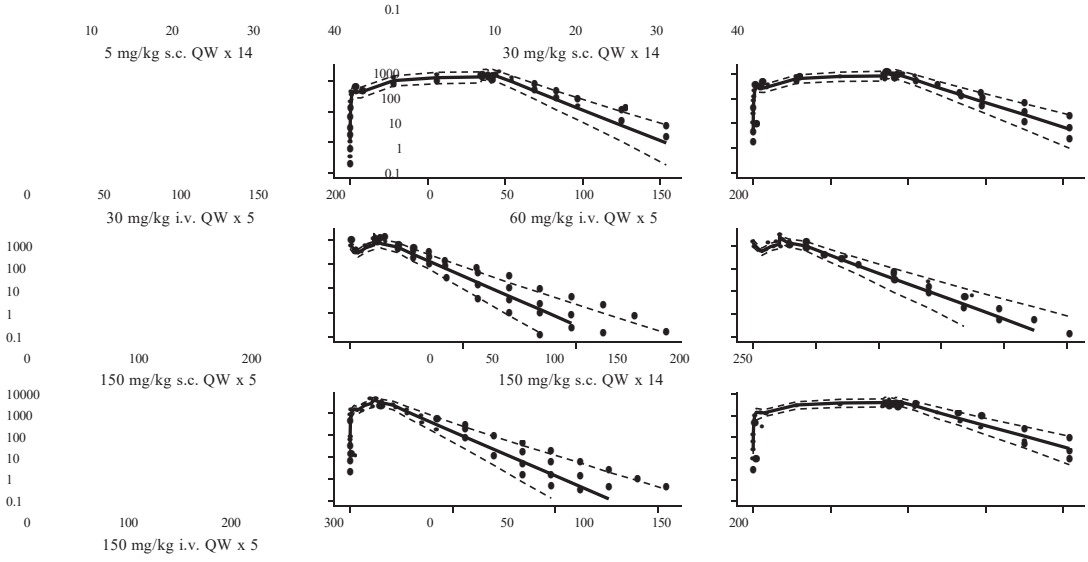

Figure 6. Visual predictive check of PK after single and multiple i.v. or s.c. administration in cynomolgus monkeys. Symbols are individual observed while solid and dashed lines represent the median and the 90% prediction interval, respectively.

(Koka et al. 2003). Similarly, a rapid reduction in NK cell count was also observed in cynomolgus monkeys after treatment with tofacitinib (CP-690550) as described above (Conklyn et al. 2004; Borie et al. 2005).

The predicted PD parameters of Hu714MuXHu for NK cell count reduction in cynomolgus monkeys indicated a potent effect of this antibody, with an estimated mean EC_{50} value of approximately 0.1 *l*g·mL^{-1} (%RSE 28.0), which is comparable to in vitro neutralization of 10 ng·mL^{-1} maca- que IL-10 by Hu714MuXHu in a PHA blast assay using cynomolgus macaque PBMCs (IC_{50} of 97 ng·mL^{-1}; data on file at Amgen Inc.). K_{in}, a measure of how fast NK cells are produced, was calculated to be 0.17 9 10^3 cells·*l*L^{-1}·day^{-1}, suggesting a rapid recovery of NK cells when IL-15 signaling pathway is no longer inhibited. This matches the observation in PK and NK cell count profiles in Figures 2 and 3. However, due to the low EC_{50} value of 0.1 *l*g·mL^{-1} and the long half-life of Hu714MuXHu, a long duration of effect was to be expected. Indeed, in the 1-month study, the NK cell number started to recover toward baseline values about 24 weeks after the last dose when the serum concentration fell below approximately1 *l*g·mL^{-1}; approaching roughly 50% recovery at the end of the study, or 334 days after the first dose, when individ- ual Hu714MuXHu concentrations were at or below the assay LLOQ of 0.1 *l*g·mL^{-1}. The PK/PD model-estimated K_{out} of 0.305 day^{-1} can be translated into an elimination half-life of 2.27 days for NK cells in monkeys. Using tofaci- tinib study data with NK cell count profiles in cynomolgus monkeys (Conklyn et al. 2004; Borie et al. 2005), and assuming an indirect response model for the NK cell deple- tion

following the administration of tofacitinib, we used the initial slope of NK cell count-time profiles to estimate K_{out} and subsequently the elimination half-life of NK cells. The estimated values of 3–4.5 days in cynomolgus mon- keys dosed with tofacitinib are generally consistent with our model-estimated NK cell elimination half-life of 2.27 days. However, caution should be exercised since we only used the initial slope for NK cell half-life estimation and did not conduct PK/PD modeling analysis on the pub- lished tofacitinib data. In addition, these comparisons were conducted between different cynomolgus monkey studies where investigational products with different targets were administered (Hu714MuXHu vs. tofacitinib).

References

Authors: Abadie and Jabri (2014). The immunopathology of celiac disease is regulated by IL-15. Immunology Review 260: 221-234.

A group of researchers including Baranda, de la Fuente, Layseca-Espinosa, Portales-Perez, Nino-Moreno, Valencia-Pacheco, and others published this in 2005. IL-15 and IL-15R in peripheral blood cells of SLE patients. The study was published in Rheumatology, volume 44, pages 1507–1513.

This sentence is a citation for a publication by Benahmed et al. (2007). An additional function for interleukin-15 (IL-15) in the dysregulation of the immune system that characterizes celiac disease: blocking TGF-beta signaling. Published in Gastroenterology, volume 132, pages 994–1008.

Along with Larson MJ, Borie DC, Si MS, Paniagua R, Higgins JP, and Changelian PS (2005). In nonhuman primates, the immunosuppressive effects of the JAK3 inhibitor CP-690,550 postpone rejection and considerably increase the survival rate of kidney allografts. Page numbers 791 to 801 in the Transplantation journal.

The authors of the 2007 study include Brendel K, Dartois C, Comets E, Lemenuel-Diot A, Laveille C, Tranchand B, and others. Have enough evaluations been conducted on population pharmacokinetic and/or pharmacodynamic models? A review of the research published between 2002 and 2004. Clinical pharmacokinetics 46: 221-234.

Andresen C, Conklyn M, Changelian P, and Kudlacz E. (2004). The NK and CD8+ T cells are specifically decreased by the JAK3 inhibitor CP-690550.

blood cell counts in cynomolgus monkeys after long-term oral administration. Volume 76, Issues 1248–1255, Journal of Leukocomics.

Along with others, Conlon KC, Lugli E, Welles HC, Rosenberg SA, Fojo AT, Morris JC (2015). This study examined the effects of recombinant human interleukin-15 on cancer patients in a first-in-human clinical trial. The results showed increased cell proliferation, redistribution, activation of CD8 T cells and natural killer cells, and cytokine production. J Medical Oncology 33: 74-82.

The authors of the 1999 study were D'Auria L, Bonifati C, Cordiali-Fei P, Leone G, Picardo M, Pietravalle M, and others. Elevated levels of serum interleukin-15 in bullous skin diseases: association with severity of illness. Published in the Journal of Arch Dermatol Research, Volume 291, Pages 354-56.

In 2009, De Nitto, Monteleone, Franze, Pallone, and Monteleone each contributed an article. Celiac disease and the gamma-chain-related cytokines interleukin-15 and interleukin-21. Article published in the World Journal of Gastroenterology on page 4609–4614.

Meibohm B, Dirks NL (2010). Kinetics of therapeutic monoclonal antibodies in a population setting. The Journal of Clinical Pharmacokinetology, 49, 636–669.

Tolomeo A. and Caligiuri M. (2001). The biology of interleukin 15 and its significance in human illness. Volume 97, Issues 14–32 of the Blood journal.

The authors of the 2004 study include Ferrari-Lacraz S, Zanelli E, Neuberg M, Donskoy E, Kim YS, Zheng XX, and others. The development and progression of illness in mouse collagen-induced arthritis may be prevented by targeting cells that express the IL-15 receptor with an antagonist mutant IL-15/Fc protein. Published in the Journal of Immunology, volume 173, pages 5818-1082.

In 2010, Gil, Park, Chung, and Park authored a paper. The release of chemokines and the proliferation of human follicular dendritic cells are both boosted by interleukin-15. Research in Immunology 130: 536-544.

Laffon A, Pascual-Salcedo D, Balsa A, Ortiz AM, Garcia-Vicuna R (2003). Serum interleukin-15 levels are

elevated in chronic rheumatoid arthritis. Chapters 639–642 of the Clinical and Experimental Rheumatology journal.
The authors of the 2011 study were Gonzalez-Alvaro, Ortiz, Alvaro-Gracia, Castaneda, Diaz-Sanchez, Carvajal, and others. In early-stage arthritic patients, blood interleukin 15 levels may foretell a harsh disease trajectory. Public Library of Science Open Access, 6(29492), 2012.
The authors of the 1994 study were Grabstein KH, Eisenman J, Shanebeck K, Rauch C, Srinivasan S, Fung V, and others. Creating an interleukin-2 receptor beta-chain-interacting T cell growth factor using cloning. Article 264: 965-968 in the Science journal.
This was published in 2010 by Haustein et al. as well as Kwun and Fechner. The blocking of the interleukin-15 receptor during kidney transplantation in non-human primates. Volume 89, Issues 937–944.
In 2004, Jamieson, Isnard, Dorfman, Coles, and Raulet published a study. Proliferation and steady-state NK cell turnover in lymphopenic areas. Johns Hopkins University Journal of Immunology, 172: 864-870.
This article was authored by Kennedy, Glaccum, Brown, Butz, Viney, Embers, and others in the year 2000. Interleukin 15–deficient animals show reversible abnormalities in the lineages of natural killer and memory CD8 T cells. Scientific American 191: 771-780.
The authors of the 2010 study were Kilkenny, Browne, Cuthill, Emerson, and Altman. The ARRIVE standards provide a framework for writing up in vivo trials using animals. Br The published article is "J Pharmacol" with the DOI number 160: 1577–1579.
The authors of the 2003 study are Koka, Burkett, Chien, Chai, Chan, Lodolce, and Lodolce. Natural killer cells that lack interleukin (IL)-15R[alpha] may survive in healthy mice, but they do not in IL-15R[alpha]-deficient animals. International Journal of Experimental Medicine 197: 977–984.
As a group, Lebrec, Horner, Gorski, Tsuji, Xia, Pan, and others published in 2013. Maintaining NK cell homeostasis in humans does not rely on IL-15. The Journal of Immunology 191: 5551–5558.
In 1998, Lodolce et al. were joined by Boone, Chai, Swain, Dassopoulos, and Trettin. The IL-15 receptor helps lymphocytes homing and proliferating, which keeps lymphoid homeostasis in check. Chapter 9: 669-676 in Immunity.
In 2000, Maiuri L, Ciacci C, Auricchio S, Brown V, Quaratino S, and Londei M published a paper. In celiac disease, interleukin 15 induces alterations in the epithelium. Journal of Gastroenterology 119: 996-1006.
In 2010, Malamut et al. were joined by Montcuquet, El Machhour, Martin-Lanneree, Dusanter-Fourt, Verkarre, and others. IL-15 may have unanticipated implications for the development of lymphomas and inflammation in celiac disease since it activates a mechanism in human intraepithelial lymphocytes that prevents cell death. Citation: J Clin Invest 120: 2131-2143.
Tough DF, Belardelli F, Mattei F, Schiavoni G (2001). When dendritic cells detect type I IFN, double-stranded RNA, or lipopolysaccharide, they secrete IL-15, which activates the cells. The Journal of Immunology 167: 1179-1187 the next year.
As published in 1997 by McInnes IB, Leung BP, Sturrock RD, Field M, and Liew FY. In RA, interleukin-15 regulates tumor necrosis factor-alpha production via T cell dependent mechanisms. The New England Journal of Medicine, 3(3), 189–195.
Cerf-Bensussan N, Meresse B, Malamut G (2012). Immunological puzzle piece: celiac disease. Vaccine 36: 907-919.

The authors of the 1998 study were Musso T, Calosso L, Zucca M, Millesimo M, Puliti M, Bulfone-Paus S, and others. In polymorphonuclear cells, interleukin-15 stimulates antibacterial and proinflammatory activities. Public Health 66: 2640-2647.
Published in 2006 by Ng CM, Lum BL, Gimenez V, Kelsey S, and Allison D. Population pharmacokinetic study supports pertuzumab fixed dose for cancer patients. Research in Pharmaceutical Sciences 23: 1275-1284.
With contributions from Ong PY, Hamid QA, Travers JB, Strickland I, Al Kerithy M, Boguniewicz M, and others (2002). Atopic dermatitis is characterized by high IgE and acute inflammation, both of which may be exacerbated by reduced IL-15. Scientific Reports 168: 505-510.
In 2003, Prlic, Blazar, Farrar, and Jameson published a paper. The homeostatic growth and in vivo

ISSN:1300-669
Volume 20 Issue 1 June 2024

persistence of natural killer cells. Journal of Experimental Medicine 197: 967–976.
In 2010, Royer et al. were joined by Pegram, Mir, Ibrahim, Villanueva, and Yin. Humanized monoclonal antibody HuHMFG1 (AS1402) population pharmacokinetics obtained from a phase I breast cancer trial. Published in the British Journal of Cancer, volume 102, pages 827–832.
Liew FY, Ruchatz H, Wei XQ, McInnes IB, and Leung BP (1998). Soluble IL-15 receptor alpha-chain administration prevents murine collagen-induced arthritis: a role for IL-15 in development of antigen-induced immunopathology. J Immunol 160: 5654–5660.
Bradley JA, Smith XG, and Bolton EM (2002). Approaches to treating organ transplant rejection by focusing on IL-15. Curr Opin Investig Drugs 3: 406–410.
Villadsen LS, Schuurman J, Beurskens F, Dam TN, Dagnaes- Hansen F, Skov L, et al. (2003). Resolution of psoriasis upon blockade of IL-15 biological activity in a xenograft mouse model. J Clin Investig 112: 1571–1580.
Waldmann TA, Tagaya Y (1999). The multifaceted regulation of interleukin-15 expression and the role of this cytokine in NK cell differentiation and host response to intracellular pathogens. Annu Rev Immunol 17: 19–49.
stig 120: 2131–2143.
Tough DF, Belardelli F, Mattei F, Schiavoni G (2001). When dendritic cells detect type I IFN, double-stranded RNA, or lipopolysaccharide, they secrete IL-15, which activates the cells. The Journal of Immunology 167: 1179-1187 the next year.
As published in 1997 by McInnes IB, Leung BP, Sturrock RD, Field M, and Liew FY. In RA, interleukin-15 regulates tumor necrosis factor-alpha production via T cell dependent mechanisms. The New England Journal of Medicine, 3(3), 189–195.
Cerf-Bensussan N, Meresse B, Malamut G (2012). Celiac disease: an immunological jigsaw. Immunity 36: 907–919. Musso T, Calosso L, Zucca M, Millesimo M, Puliti M, Bulfone-Paus S, et al. (1998). Interleukin-15 activates proinflammatory and antimicrobial functions in polymorphonuclear cells. Infect Immun 66: 2640–2647.
Ng CM, Lum BL, Gimenez V, Kelsey S, Allison D (2006). Rationale for fixed dosing of pertuzumab in cancer patients based on population pharmacokinetic analysis. Pharm Res 23: 1275–1284.
Ong PY, Hamid QA, Travers JB, Strickland I, Al Kerithy M, Boguniewicz M, et al. (2002). Decreased IL-15 may contribute to elevated IgE and acute inflammation in atopic dermatitis. J Immunol 168: 505–510.
Prlic M, Blazar BR, Farrar MA, Jameson SC (2003). In vivo survival and homeostatic proliferation of natural killer cells. J Exp Med 197: 967–976.
Royer B, Yin W, Pegram M, Ibrahim N, Villanueva C, Mir D, et al. (2010). Population pharmacokinetics of the humanised monoclonal antibody, HuHMFG1 (AS1402), derived from a phase I study on breast cancer. Br J Cancer 102: 827–832.
Ruchatz H, Leung BP, Wei XQ, McInnes IB, Liew FY (1998). Soluble IL-15 receptor alpha-chain administration prevents murine collagen-induced arthritis: a role for IL-15 in development of antigen-induced immunopathology. J Immunol 160: 5654–5660.
Smith XG, Bolton EM, Bradley JA (2002). Targeting IL-15 as a therapeutic strategy in organ transplant rejection. Curr Opin Investig Drugs 3: 406–410.
Villadsen LS, Schuurman J, Beurskens F, Dam TN, Dagnaes- Hansen F, Skov L, et al. (2003). Resolution of psoriasis upon blockade of IL-15 biological activity in a xenograft mouse model. J Clin Investig 112: 1571–1580.
Waldmann TA, Tagaya Y (1999). The multifaceted regulation of interleukin-15 expression and the role of this cytokine in NK cell differentiation and host response to intracellular pathogens. Annu Rev Immunol 17: 19–49.